CrossMark

Sub-decadal North Atlantic Oscillation variability in observations and the Kiel Climate Model

Annika Reintges[1] · Mojib Latif[1,2] · Wonsun Park[1]

Abstract The North Atlantic Oscillation (NAO) is the dominant mode of winter climate variability in the North Atlantic sector. The corresponding index varies on a wide range of timescales, from days and months to decades and beyond. Sub-decadal NAO variability has been well documented, but the underlying mechanism is still under discussion. Other indices of North Atlantic sector climate variability such as indices of sea surface and surface air temperature or Arctic sea ice extent also exhibit pronounced sub-decadal variability. Here, we use sea surface temperature and sea level pressure observations, and the Kiel Climate Model to investigate the dynamics of the sub-decadal NAO variability. The sub-decadal NAO variability is suggested to originate from dynamical large-scale air-sea interactions. The adjustment of the Atlantic Meridional Overturning Circulation to previous surface heat flux variability provides the memory of the coupled mode. The results stress the role of coupled feedbacks in generating sub-decadal North Atlantic sector climate variability, which is important to multiyear climate predictability in that region.

✉ Annika Reintges
areintges@geomar.de

[1] GEOMAR Helmholtz Centre for Ocean Research Kiel, Düsternbrooker Weg 20, 24105 Kiel, Germany

[2] University of Kiel, Kiel, Germany

1 Introduction

The North Atlantic Oscillation (NAO) is a large-scale seesaw in atmospheric mass between the Azores high and the Icelandic low (Hurrell 1995; Visbeck et al. 2001; Hurrell et al. 2003). Variations in the NAO are associated with strong changes in wintertime storminess over the North Atlantic, and European and North American surface air temperature (SAT) and precipitation, and thus have major economic impacts. A statistically significant sub-decadal peak can be identified in the power spectrum of the traditional NAO index (Czaja and Marshall 2001; Fye et al. 2006). Statistically significant sub-decadal peaks are also seen in the power spectra of other quantities observed in the North Atlantic sector (Deser and Blackmon 1993; Sutton and Allen 1997; Czaja and Marshall 2001; Fye et al. 2006; Álvarez-García et al. 2008).

The sub-decadal variability in the North Atlantic sector is distinct from the longer-term multidecadal variability in that region (Álvarez-García et al. 2008), which is associated with the Atlantic Multidecadal Oscillation/Variability (AMO/V) (Knight et al. 2005). In this study, we only address the sub-decadal variability. Different competing hypotheses have been put forward to explain the North Atlantic sector sub-decadal variability. It has been linked, for instance, to Arctic sea ice (Deser and Blackmon 1993), to advection by the mean ocean circulation (Sutton and Allen 1997), to the wind-driven ocean circulation (Czaja and Marshall 2001; Marshall et al. 2001), to the Atlantic Meridional Overturning Circulation (AMOC) (Eden and Greatbatch 2003; Álvarez-García et al. 2008), and to stochastic resonance (Saravanan and McWilliams 1997, 1998). Further, it is controversial whether the North Atlantic sub-decadal climate variability observed in different variables is part of *one* single dynamical mode of the

coupled ocean–atmosphere–sea ice system or is composed of *different* modes each originating from different physical processes.

Here, we investigate the origin of the sub-decadal NAO variability and related climate variability in the North Atlantic sector by analyzing historical observations and a millennial control integration of the Kiel Climate Model (KCM), a coupled ocean–atmosphere–sea ice general circulation model. By definition, time-varying external forcing is not considered in such control integration and variability is only internally generated. Section 2 provides information about the observational data, the climate model and the experimental setup, and the statistical method for the identification of the sub-decadal mode in the different datasets. In Sect. 3, by jointly discussing the observations and the results from the KCM, we present the mechanism that is suggested to produce the sub-decadal NAO variability. Summary of the major findings and main conclusions are presented in Sect. 4.

2 Data and methodology

2.1 Observational data

We use the observed station-based winter (December through March, DJFM) NAO index during 1864–2014 from https://climatedataguide.ucar.edu/climate-data/hurrell-north-atlantic-oscillation-nao-index-station-based. The station-based NAO index is defined as the difference of the normalized sea level pressure (SLP) anomaly time series between Lisbon (Portugal; 38.72°N, 9.17°W) and Stykkisholmur/Reykjavik (Iceland; 65.07°N, 22.72°W). The climate model's NAO index is computed in an analogous manner from the nearest grid points. The station-based index also well describes the model's NAO variability (see supplementary Fig. S1).

In the regression and cross-correlation analyses presented below, gridded sea surface temperatures (SSTs, ERSST V3b) provided for January 1854–April 2015 are from http://www.ncdc.noaa.gov/ersst. A dipolar SST index is defined from the observed SSTs by subtracting mid-latitudinal from subpolar North Atlantic SST anomalies (see boxes in Fig. 1b; according to this convention, a negative index means an enhanced meridional SST gradient). The KCM's dipolar SST index is computed in an analogous manner.

Gridded sea level pressure data (SLPs, HadSLP2) provided for the time period January 1850–December 2014 is obtained from http://www.metoffice.gov.uk/hadobs/hadslp2/. The common period 1864–2014 is used when computing correlations and regressions of the SSTs and SLPs with respect to the NAO index. Measurements of the AMOC index at 26.5°N from the RAPID array are

downloaded from http://www.rapid.ac.uk/rapidmoc/ (Smeed et al. 2015). The RAPID data have been widely used during the recent years; for example, by Bryden et al. (2014) and Cunningham et al. (2013), two studies which are relevant here. The AMOC index is provided for the period April 2004–March 2015. We use the annual mean values of the AMOC index for the eleven years during 2004–2014.

2.2 Coupled model and experiments

The Kiel Climate Model (KCM; see Park et al. 2009) is an atmosphere–ocean–sea ice general circulation model. It consists of the ECHAM5 atmosphere general circulation model on a T31 horizontal grid (3.75° × 3.75°) with 19 vertical levels, which is coupled through the OASIS coupler to the NEMO ocean-sea ice model on a 2° Mercator mesh amounting on average to 1.3° resolution. Enhanced meridional resolution of 0.5° is employed in the equatorial region and the ocean model is run with 31 levels. The KCM has been used in many climate variability and response studies. A list of studies conducted with the KCM can be obtained from http://www.geomar.de/en/research/fb1/fb1-me/research-topics/climate-modelling/kcms/. We analyze the last 700 years of output from a millennial present-day control simulation after skipping the first 300 years, which has been initialized with Levitus climatology. The climatology of selected quantities is shown in Fig. 1. Like many other climate models, the KCM suffers from large biases in the North Atlantic region (see supplementary Fig. S2 and S3). In particular, a cold SST bias is observed in the mid-latitudes, which largely originates from an incorrect path of the North Atlantic Current (Drews et al. 2015). We additionally investigate 700 years from an integration of the ECHAM5 atmosphere general circulation model coupled to a slab ocean model with a constant depth of 50 m. In this reduced coupled model, changes in ocean circulation are completely ignored. Comparison of the fully coupled (KCM) integration with the slab ocean coupled integration provides information about the importance of ocean dynamical feedbacks for the sub-decadal NAO variability in the KCM.

Finally, the ECHAM5 model version employed by the KCM is integrated in an uncoupled mode with prescribed SSTs. Two experiments are performed, each 99 years long. The first experiment is a control run in which only the observed monthly SST climatology drives the model. In the second experiment, the observed winter (DJFM) SST anomalies associated with the positive phase of the sub-decadal NAO mode (see Fig. 7a, right panel) are superimposed on the observed SST climatology globally. The differences between the two experiments provide information
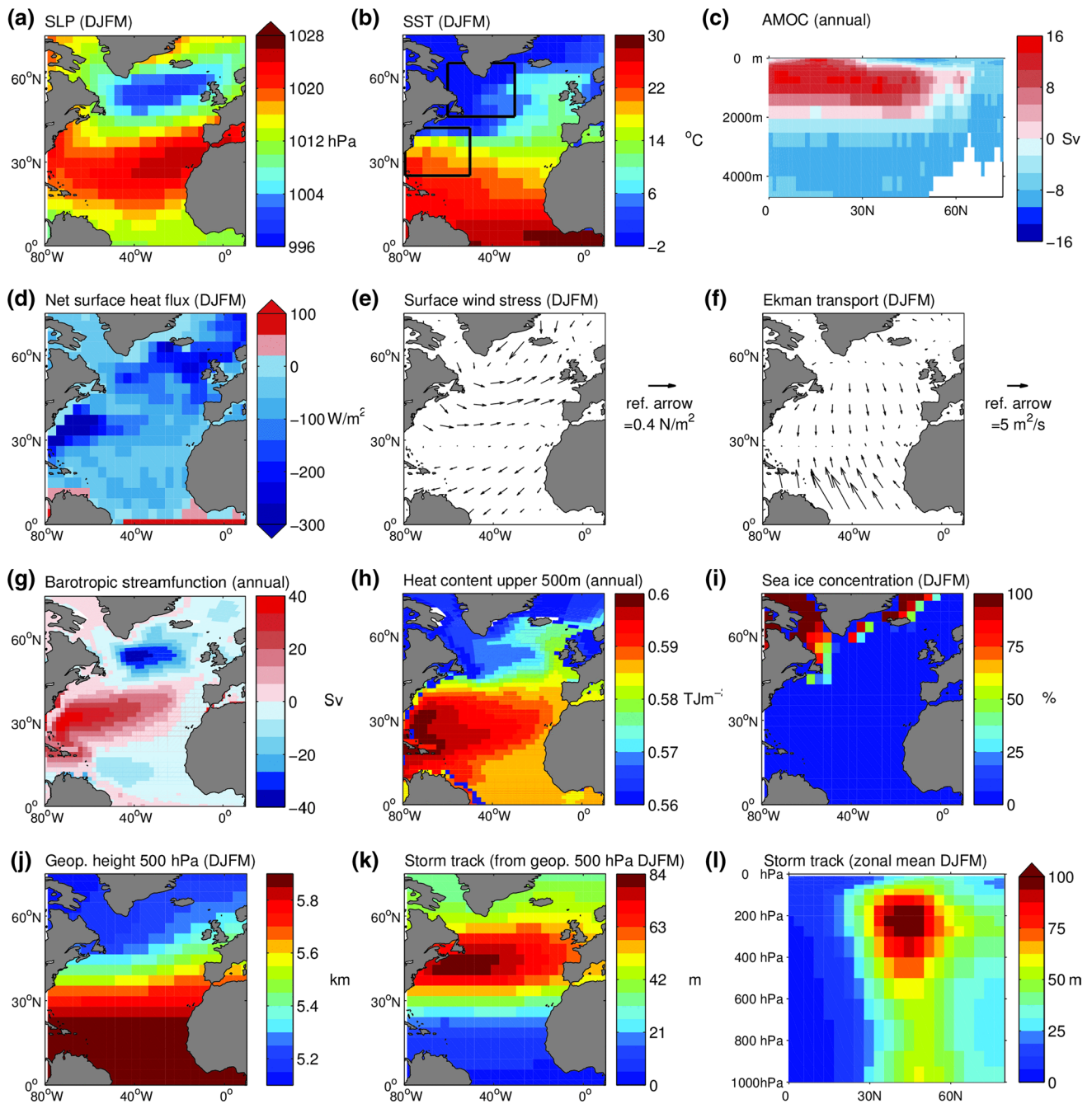
Fig. 1 Climatology of selected quantities averaged over the last 700 years of the millennial control integration of the KCM. **a** SLP (DJFM). **b** SST (DJFM). **c** Atlantic Meridional Overturning streamfunction (annual). **d** Net surface heat flux (DJFM). **e** Surface wind stress (DJFM). **f** Ekman transport (DJFM). **g** Barotropic streamfunction (annual means). **h** Upper ocean (0–500 m) heat content (annual means referenced to 0 K). **i** Sea ice concentration (DJFM). **j** 500 hPa geopotential height (DJFM). **k** Storm track based on the 500 hPa geopotential height (DJFM). **l** Atlantic (80°W–10°E) zonal mean storm track based on the geopotential height (DJFM). In (**b**), the *two boxes* indicate the areas over which data have been averaged to calculate the dipolar SST index (SSTs in *subpolar box* minus SSTs in *subtropical box*; used in the Figs. 4, 5)

about whether and how the SST anomalies feed back onto the atmosphere and thus yield some information about the role of air-sea coupling in generating the sub-decadal NAO mode. The atmospheric response is defined as the difference between the two long-term means (experiment minus control), where the long-term mean is computed from all 99 DJFM values. A *t*-test provides the statistical significance of the response.

2.3 Statistical methods

Singular Spectrum Analysis (SSA; see Vautard and Ghil 1989) is applied here to derive oscillatory modes from the observations and the model data. The results of the SSA may be sensitive to the choice of parameters. In order to investigate such sensitivity different variables and window lengths have been applied, and the results are rather robust. In the SSAs of the observed NAO index and the observed (dipolar) SST index, both covering about 150 years, the window length is 15 years and only these results are shown below. Sensitivity tests using a window length of 20 years were performed. The results are virtually unchanged, suggesting robustness in the results from the observational analyses. Furthermore, sub-decadal modes are identified from SSA applied separately to the observed NAO index and the observed (dipolar) SST index. With regard to the KCM, SLP, geopotential, storm track, SST, surface heat flux and AMOC indices from the model have been individually used in the SSA, and they all yield the same sub-decadal period of 9 years. KCM-results shown below are from SSAs employing a window length of 100 years. Sensitivity tests conducted using several window lengths in the range of 70–150 years yield similar results. Thus, we can confidently state that at least in the model, a statistically significant sub-decadal mode is simulated in the North Atlantic sector that has expressions in both the atmosphere and the ocean.

Cross-correlation and linear regression analyses were performed to investigate the links between different variables. In the calculation of the confidence limits for the correlation coefficients, we use a *t*-test based on the effective number of degrees of freedom which is estimated from the decorrelation time of each time series (Leith 1973) separately, explaining the differing confidence limits in the plots shown below. The decorrelation time is defined here as the e-folding timescale of the time series' auto-correlation function. By multiplying the critical correlation coefficient with the standard deviation of the variable under consideration we obtain the threshold for the corresponding regression coefficient.

3 Results

3.1 Statistical analyses

We first compute the power spectrum of the observed winter-NAO index during 1864–2014. Sub-decadal NAO variability is statistically significant at the 99 %-confidence level in the observations (Fig. 2a), which is one of the main motivations for this study. We next computed the
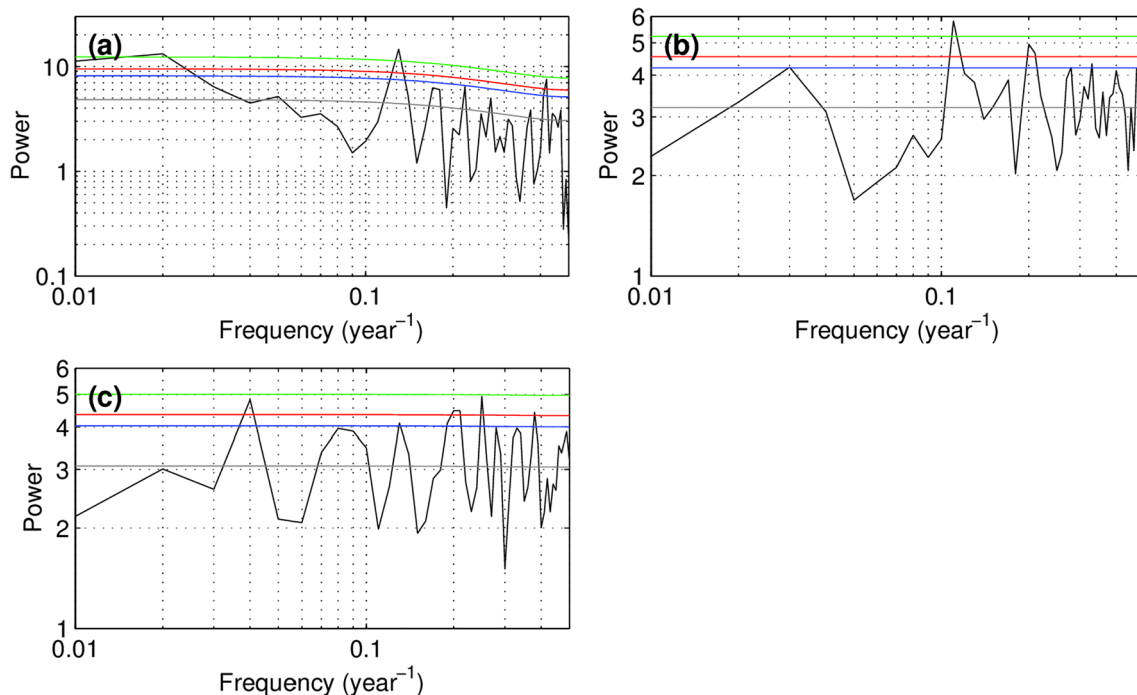

Fig. 2 Power spectra of the NAO index calculated from **a** the observations during 1864–2014, **b** the coupled KCM integration employing a dynamical ocean, **c** the coupled KCM run employing a slab ocean model. A Hamming window with a length of 100 years is used. The *thin grey horizontal line* indicates the median spectrum of a red noise (**a**) or white noise (**b**, **c**) process. Confidence limits are shown for 90 % (*blue*), 95 % (*red*), and 99 % (*green*)
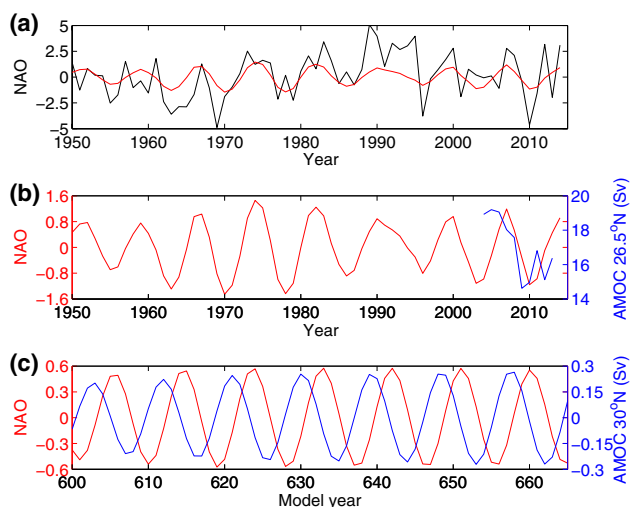
Fig. 3 Time series of the NAO index during winter (DJFM) and the AMOC index (annual means). **a** Observed NAO index (*black*) and its reconstruction using the sub-decadal SSA mode derived from the period 1864–2014 (*red*). **b** Sub-decadal mode reconstruction of the observed NAO index (*red*, reproduced from **a**) and the AMOC strength at 26.5°N from the RAPID measurements provided for the period 2004–2013 (*blue*). **c** Sub-decadal mode reconstruction of the NAO index (*red*) and the AMOC strength at 30°N (*blue*) from the KCM

winter-NAO index spectra from the two coupled model simulations. Differences in the spectra computed from the two simulations depict the role of ocean dynamics in influencing the NAO. Statistically significant sub-decadal NAO variability is observed in the power spectrum of the coupled simulation employing a dynamical ocean model (Fig. 2b), the KCM, but not in that of the coupled integration with the slab ocean model (Fig. 2c). The existence (absence) of the sub-decadal NAO mode in the power spectrum computed from the coupled simulation with the dynamical (slab) ocean model was verified by repeating the spectral analysis with different window types and window lengths. On the contrary, the peaks seen at 25 and 4 years in Fig. 2c are not robust. The lack of enhanced sub-decadal NAO variability in the coupled simulation with the slab ocean model suggests that dynamical ocean processes, through their influence on SST, is essential to produce the sub-decadal NAO mode in the KCM. We return to this point below.

Consistent with the power spectrum presented above (Fig. 2a), the SSA of the observed winter-NAO index of 1864–2014 reveals a sub-decadal oscillatory mode with a period of 8 years (red line in Fig. 3a, b) that accounts for 18 % of the total variance (Fig. 4a). This SSA mode is, however, not statistically significant against red noise at the 95 % confidence limit. We present the reconstructed NAO index together with the AMOC index at 26.5°N from the RAPID array in Fig. 3b. The evolution of the observed

AMOC index depicts similar sub-decadal variability (Bryden et al. 2014; Cunningham et al. 2013) as the reconstructed NAO index. However, the AMOC record is very short only covering about a decade, which does not allow drawing any inferences about causality and the reason for additionally investigating the sub-decadal NAO variability simulated by the KCM. As will be discussed in detail below, the KCM depicts a close connection between the AMOC and the NAO at sub-decadal timescales (Fig. 3c) such that the former leads the latter by about a year. This suggests the assumption that the observed sub-decadal AMOC signal is part of an oscillation in the North Atlantic region and related to the NAO.

We next perform SSA on the KCM's NAO index, which yields a leading oscillatory sub-decadal mode with a period of 9 years (red line in Fig. 3c) accounting for about 4 % of the total variance (Fig. 5a). We note that the explained variance strongly depends on the window length, while the existence of the sub-decadal SSA mode does not. When choosing a window length of 15 years, as in the observational analyses, the explained variance is similar to that obtained from the SSA of the observed NAO index. For example, using only the last 150 years from the model and a window length of 15 years yields a sub-decadal NAO mode that accounts for about 20 % of the variance. Further, since SSA provides modes which are sharply peaked in frequency space, the variance accounted for by SSA modes is generally considerably lower in comparison to other statistical techniques such as Empirical Orthogonal Function (EOF) analysis which covers a larger frequency range. The sub-decadal NAO mode obtained from the KCM (Fig. 3c) is statistically significant against red noise at the 95 % confidence limit. We observed in the KCM a strong amplitude modulation of the sub-decadal NAO variability on centennial timescales (red curve in Fig. 5b). No sub-decadal mode is obtained from the SSA of the NAO index simulated in the coupled integration with the slab ocean model (not shown), which reinforces the findings from the investigation of the power spectra (Fig. 2). In the coupled experiment in which the dynamical ocean model is replaced by a slab ocean model, the NAO index does not exhibit statistically significant sub-decadal variability above the background spectrum (Fig. 2c). Furthermore, applying SSA to the NAO index does not reveal a statistically significant sub-decadal NAO mode. However, a peak at multidecadal timescales is seen in the spectrum of the NAO index obtained from the coupled integration with the slab ocean. This peak appears not to be robust, because it is neither supported by SSA nor seen in the power spectra of other variables (not shown). The comparison of the KCM results with those of the coupled slab ocean model integration demonstrates that ocean dynamical processes are necessary to produce the sub-decadal NAO mode in the KCM.
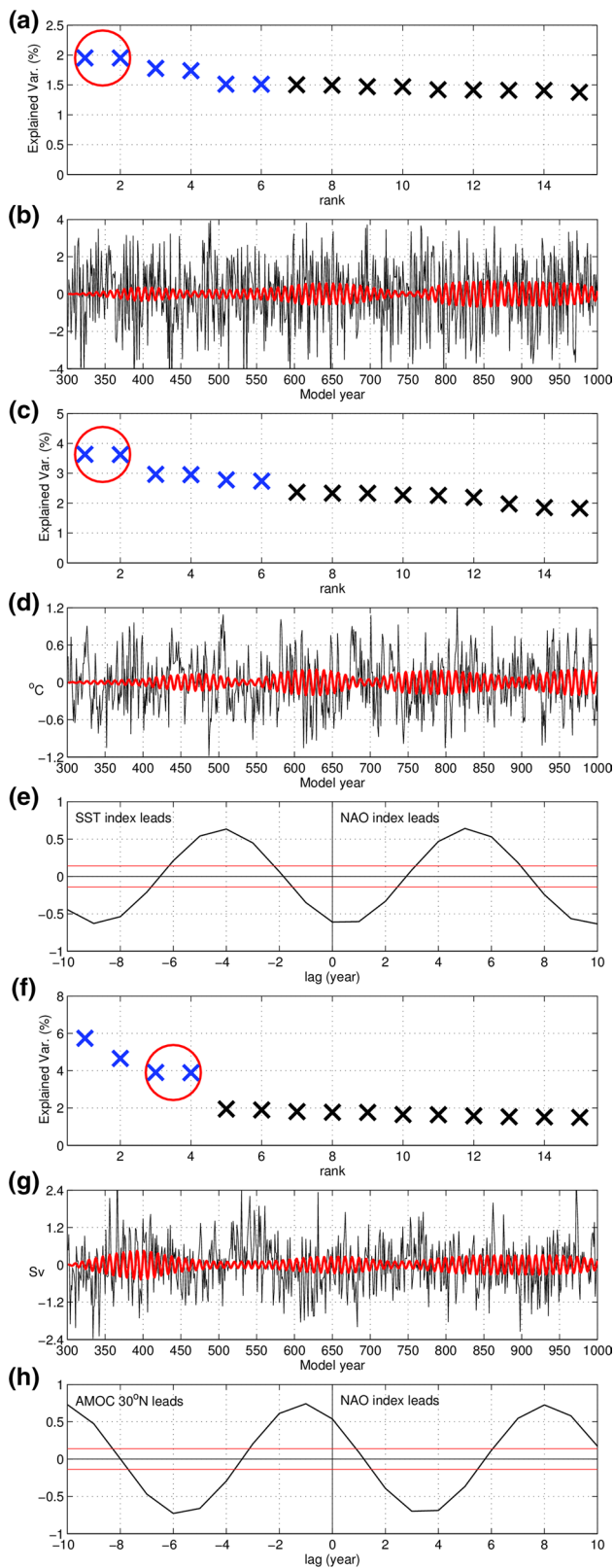
Fig. 4 Singular Spectrum Analyses (SSAs) applied to observed variables during winter (DJFM). **a**, **b** Results for the NAO index 1864–2014, **c**, **d** for the dipolar SST index 1855–2015. Eigenvalue spectra are shown in (**a**) and (**c**). The sub-decadal eigenvalue pair is marked by the *red circle*. *Blue crosses* indicate eigenvalues that are statistically significant (95 %-confidence limit) based on a Monte Carlo test against red-noise and 1000 realisations. The raw time series (*thin black line*) and the SSA reconstruction using the sub-decadal eigenvalue pair (*thick red line*) are shown in (**b**) and (**d**). The cross-correlation between the sub-decadal mode reconstructions of the NAO and the dipolar SST index calculated over the period 1864–2014 is shown in (**e**). The *red horizontal lines* indicate the 95 %-confidence interval. Depending on the time lag, the time series provide 45–48 effective degrees of freedom
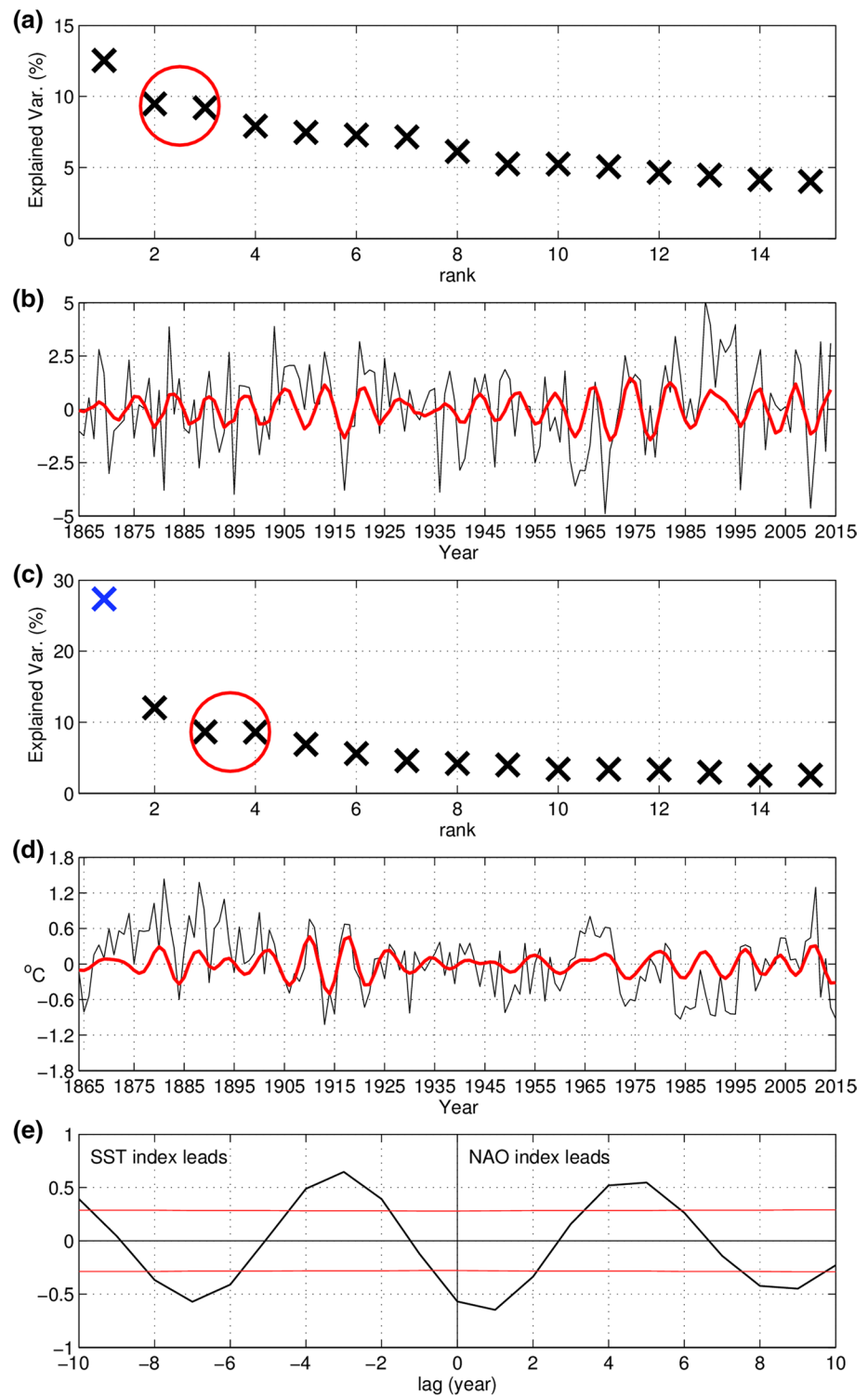
3.2 Sub-decadal mode surface patterns

The sub-decadal NAO-index reconstructions are used as indices to compute regression patterns of SLP anomalies during winter (DJFM) from the observations and the KCM. Both evolutions, that obtained from observations (Fig. 6a)

and that from the KCM (Fig. 6b), depict a transition from the negative polarity of the NAO at lag −4 yr to its positive polarity at lag 0 yr. At lag −2 yr, SLP anomalies are considerably weaker, so that the sub-decadal SLP variability approximately takes the form of a standing oscillation in the observations and in the KCM. Notable differences between

◄**Fig. 5** Singular Spectrum Analyses (SSAs) applied to variables from the KCM (700 years). **a–e** Analogous to Fig. 4a–e; SSA results for the AMOC index at 30°N are shown in (**f**) and (**g**); cross-correlations between the sub-decadal mode reconstructions of the NAO index and the AMOC index in (**h**). In (**e**), the number of effective degrees of freedom is 193, in (**h**) 200

similar, supporting that the model is reasonably well capturing the observed sub-decadal SLP variability.

Lag-regressions of sea surface temperature (SST) anomalies during DJFM are computed next (Fig. 7), again upon the two NAO-index reconstructions. In both the observations (Fig. 7a) and the KCM (Fig. 7b), negative SST anomalies appear in the mid-latitudes at lag −4 yr, which intensify during the subsequent 2 years. In the Labrador and Irminger Seas, negative SST anomalies emerge at lag −1 yr in both datasets (not shown). At lag 0 yr, i.e. when the sub-decadal NAO mode is in its positive phase, the negative SST anomaly in the subpolar North Atlantic has strengthened, while in the mid-latitudes, the negative SST anomaly is replaced by a positive SST anomaly which emanated from the western boundary.

3.3 Mechanism in the KCM

In order to gain further insight into the mechanism behind the sub-decadal NAO variability, we now investigate the model results in more detail. Consistent with observations (Czaja 2001; Cayan 1992), the net surface heat flux anomalies (Fig. 8a) tend to drive the SST anomalies in the subpolar and mid-latitude North Atlantic during the two extreme phases (lag −4 yr, lag 0 yr) of the sub-decadal NAO mode. At these lags, the anomalous wind stress (Fig. 8b) through its curl forces anomalous Ekman transports (Fig. 8c), and these contribute to the generation of the SST anomalies in the centers of action. At lag −3 yr (not shown) and lag −2 yr, the net heat flux anomalies, though not being statistically significant, still tend to damp the SST anomalies, especially in the mid-latitude North Atlantic. Furthermore, wind stress anomalies are weak in this transition phase of the sub-decadal NAO mode (Fig. 8b). Thus, the strong negative SST anomalies simulated by the KCM at lag −2 yr must originate from ocean dynamical processes. The barotropic streamfunction anomalies associated with the sub-decadal NAO mode depict statistically significant regressions at all lags (Fig. 8d). An "intergyre" gyre (Marshall et al. 2001) develops at lag −4 yr and persists until lag −2 yr, pushing the subpolar-gyre boundary southward. This favors sea surface cooling in the mid-latitudes with a time delay of 1 to 2 years, which constitutes a positive feedback on the SST anomalies in that region.

A delayed negative feedback is provided by the AMOC which responds to the dipolar heat flux anomalies

the SLP regression patterns are also seen, especially at lag −2 yr. However, this mostly concerns non-significant features. The gross features of the time–space structure are

Fig. 6 Lag-regressions of sea level pressure (SLP) anomalies during winter (DJFM) upon the sub-decadal mode of the NAO index. **a** From observations (Hurrell NAO index and HadSLP2 during 1864–2014). **b** From the KCM (700 years). *Hatching* denotes statistical significance at the 95 %-confidence level. Please note the different scales
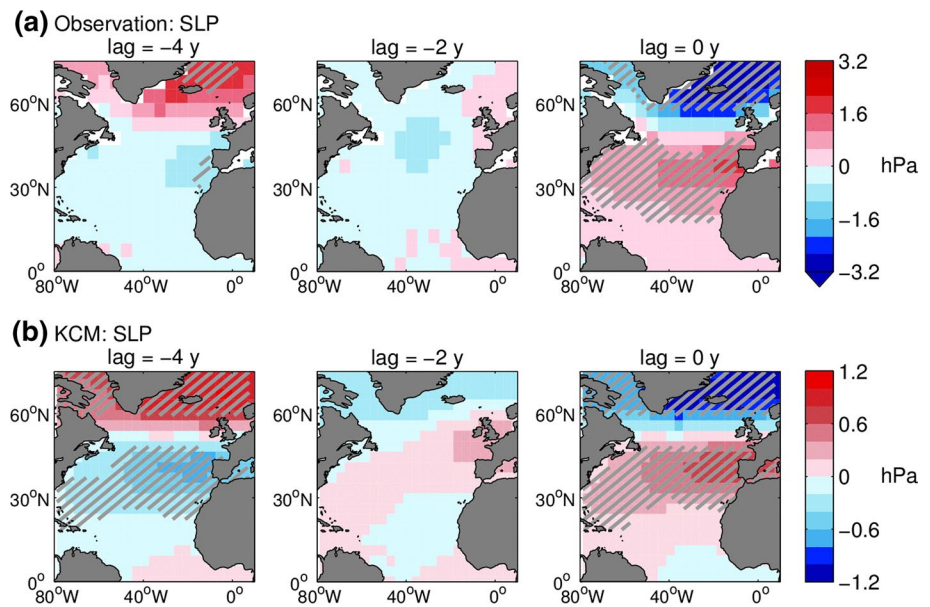

Fig. 7 Lag-regressions of sea surface temperature (SST) anomalies during winter (DJFM) upon the sub-decadal mode of the NAO index. **a** From observations (ERSST V3b during 1864–2014). **b** From the KCM (700 years). *Hatching* denotes statistical significance at the 95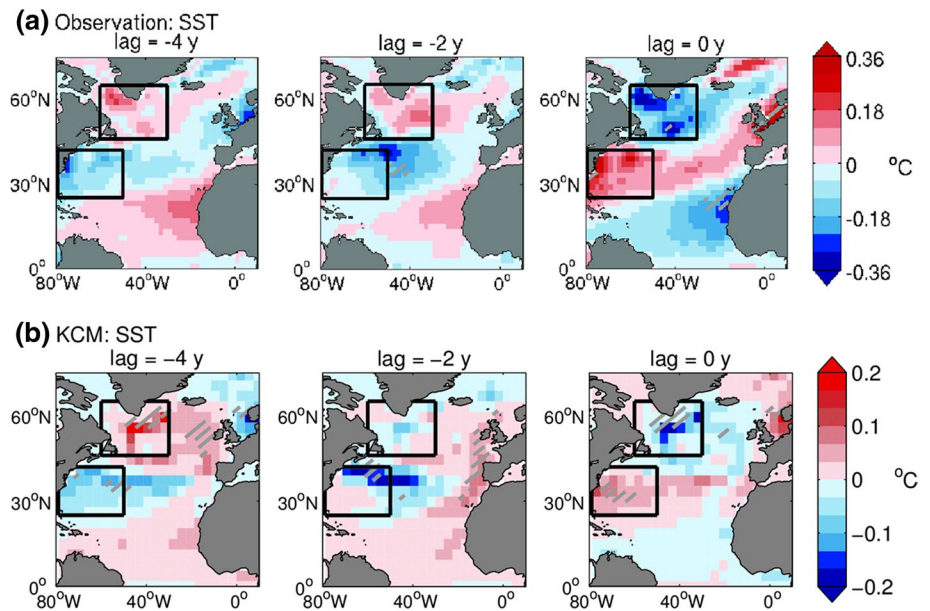 % confidence level. Please note the different scales. The *two boxes* indicate those areas over which data have been averaged to calculate the dipolar SST index (*subpolar box* minus *subtropical box*) used in the Figs. 4 and 5

prevailing during the negative extreme of the sub-decadal NAO mode at lag −4 yr (Fig. 8a). Statistically significant upper ocean (0–500 m) heat content anomalies (Fig. 8e) are simulated by the model in the mid-latitudes at lag −4 yr. At lag −2 yr, a small heat content signal of opposite sign develops in the west and follows the path of the KCM's North Atlantic Current, eventually reversing the SST tendency in the mid-latitude North Atlantic. This heat content signal is attributed to the concurrent changes in the AMOC. The overturning streamfunction depicts a well-developed dipolar anomaly with a node near 45°N at lag−2 yr (Fig. 9). The positive AMOC anomaly centered near 30°N enhances the transport of warm water in the upper ocean

from the subtropics to the mid-latitudes. Further to the north, negative SST and heat content anomalies develop at lag −1 yr (not shown) and reach full strength at lag 0 yr (Figs. 7, 8). At this time, we find increased sea ice concentration in the western subpolar North Atlantic (Fig. 8f).

To sharpen the role of the AMOC in the KCM's sub-decadal NAO variability, SSA was performed on an AMOC index defined as the maximum overturning streamfunction at 30°N (black curve in Fig. 5g). The leading oscillatory SSA mode, comprising basin-wide changes of the AMOC (not shown), is multidecadal (Park and Latif 2008) (rank 1 and 2 in Fig. 5f) and not of relevance here. The next energetic SSA mode accounting for about 8 % of the

Fig. 8 Lag-regressions upon the leading oscillatory (sub-decadal) SSA mode of the NAO index calculated from the KCM. **a** Net surface heat flux (DJFM). **b** Surface wind stress (DJFM). **c** Ekman transport (DJFM). **d** Barotropic streamfunction (annual means; climatology overlaid as solid contours for positive and dashed contours for negative values, contour interval of 5×10^6 m^3/s). **e** Upper ocean (0–500 m) heat content (annual means). **f** Sea ice concentration anomalies (DJFM). Statistical significance at the 95 % confidence level is indicated by hatching in (**a**) and (**d**)–(**f**), and by *red arrows* in (**b**) and (**c**)
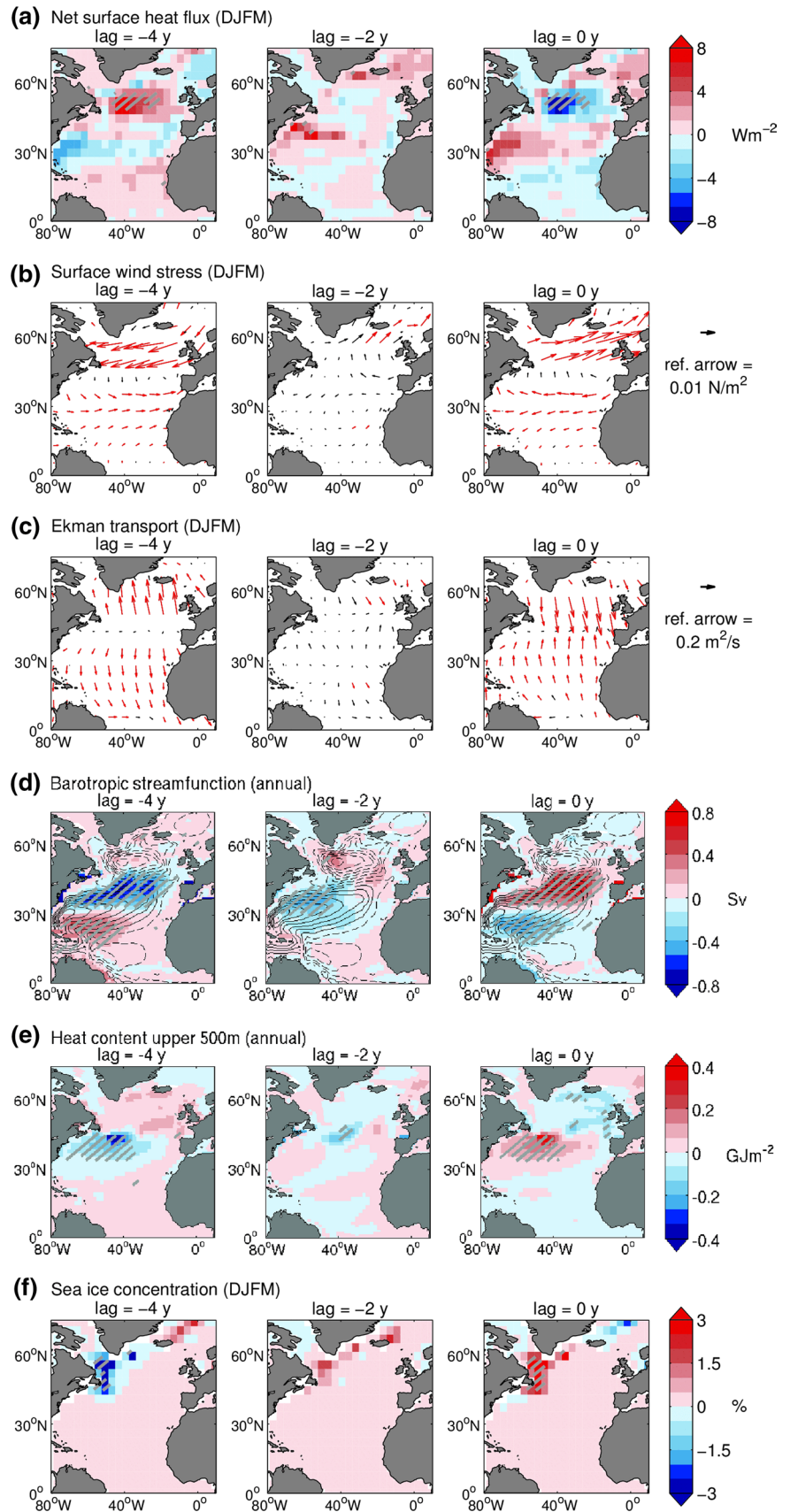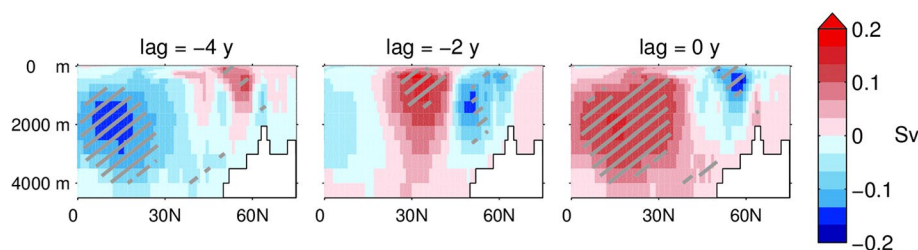
Fig. 9 Lag-regressions of the Atlantic meridional overturning streamfunction upon the leading oscillatory (sub-decadal) mode of the NAO index calculated from the KCM (700 years). *Hatching* denotes statistical significance at the 95 %-confidence level

total variance is significant against a red noise process and sub-decadal (Fig. 5f, g) with a period of 9 years. We reconstructed the AMOC index using this SSA mode (red curve in Fig. 5g) and lag-correlated the reconstructed AMOC index with the sub-decadal NAO index reconstruction (red curve in Fig. 5b). The two indices, which have been derived from independent statistical analyses, are strongly lag-correlated (Fig. 5h), suggesting they are part of the same physical mode. The largest correlation (r = 0.74) is attained when the (reconstructed) AMOC index leads the (reconstructed) NAO index by 1 year (see also Fig. 3c). This suggests that the AMOC is instrumental, through its impact on SST, in driving the sub-decadal NAO variability in the KCM.

3.4 Air–sea coupling

Conceptually, the sub-decadal variability simulated by the KCM can be understood as a delayed action oscillator (Marshall et al. 2001). We hypothesize that the dipolar overturning anomaly, with a time delay, strengthens the meridional SST gradient between the subpolar and mid-latitude North Atlantic. This in turn drives the phase change of the sub-decadal NAO mode to its positive polarity. To test this hypothesis a dipolar SST index is calculated from both the observations and the model by subtracting mid-latitudinal from subpolar SST anomalies (the SSTs were averaged over the boxes shown in Figs. 1b, 7). According to this definition, a stronger meridional SST gradient is associated with a negative index. SSA applied to the dipolar SST indices calculated from the observations and the model yields sub-decadal modes with the same periods as those obtained from the SSA of the NAO indices (Figs. 4c, d, 5c, d), lending further support to the assumption that the sub-decadal oscillation is a robust mode in both the observations and the model. We correlate next the sub-decadal SSA-mode reconstructions of the dipolar SST indices with the sub-decadal SSA-mode reconstructions of the NAO indices (Figs. 4b, 5b). The cross-correlation functions calculated from the observations (Fig. 4e) and the model (Fig. 5e) are very similar. They both clearly depict the sub-decadal periodicity and exhibit statistically significant negative cross-correlation (above the 95 % level) at lag 0 yr. This supports the conjecture that the sub-decadal NAO variability
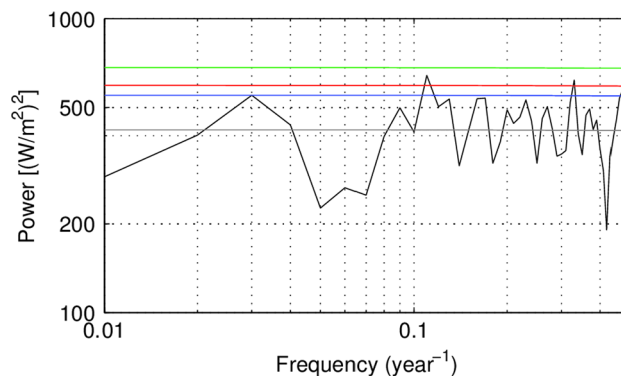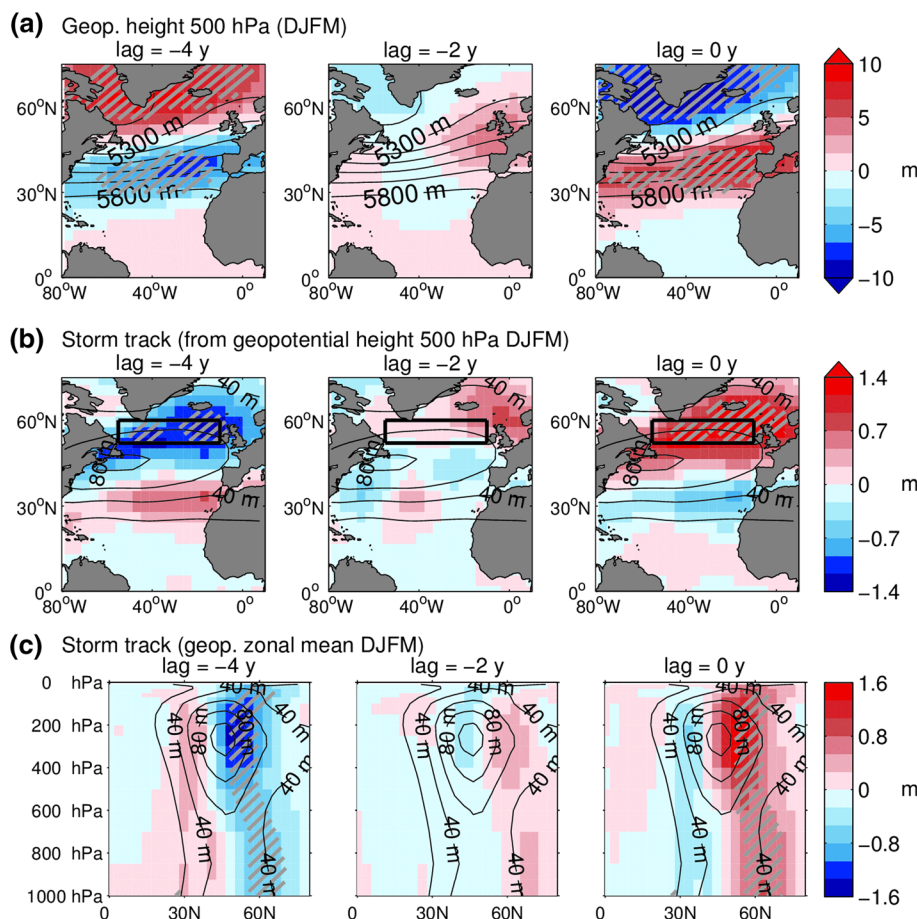

Fig. 10 Power spectrum of the heat flux index (averaged over the subpolar North Atlantic, 48°–15°W/43°–58°N) calculated from the KCM. A Hamming window with a length of 100 years is used. The *thin grey horizontal line* indicates the median spectrum of a red noise process. Confidence limits are shown for 90 % (*blue*), 95 % (*red*), and 99 % (*green*)

involves large-scale ocean–atmosphere coupling, with a stronger meridional SST gradient driving a stronger NAO index and vice versa.

As shown in Fig. 5, the dipolar SST index and NAO index SSA-mode reconstructions are highly correlated. The fact that a sub-decadal periodicity can be identified in the NAO index by itself supports the notion that the sub-decadal NAO variability is part of a coupled ocean–atmosphere mode, assuming that the atmosphere by itself does not produce a sub-decadal cycle. The atmospheric response to mid-latitudinal SST anomalies is a controversial topic and not well understood. This is demonstrated, for example, by the diversity of model results. The coarse horizontal resolution (T31) of the atmospheric component (ECHAM5) of the KCM does not a priori inhibit the atmosphere model to responding to the dipolar SST anomalies. The spatial scale of the dipolar SST anomaly, exhibiting opposite changes in the subpolar and mid-latitudinal Atlantic, is sufficiently large to be resolved by the atmosphere model.

One needs to bear in mind in this context that consistent with observations, a positive phase of the NAO is associated with surface heat flux anomalies (Fig. 8a, right panel) which tend to cool the subpolar North Atlantic and warm the region to the south of it. These heat flux anomalies reinforce the dipolar SST anomaly in the KCM, constituting a positive

Fig. 11 Lag-regressions upon the leading oscillatory (sub-decadal) SSA mode of the NAO index calculated from the KCM. **a** 500 hPa geopotential height (DJFM). **b** Storm track based on the 500 hPa geopotential height (DJFM). **c** Atlantic (80°W–10°E) zonal mean storm track based on the geopotential height (DJFM). Statistical significance at the 95 % confidence level is indicated by *hatching*

feedback. Consistent with the spectral analyses presented above, the power spectrum of the heat flux anomalies averaged over the subpolar North Atlantic (48°–15°W/43°–58°N) depicts a peak at 9 years that is statistically significant at the 99 % level (Fig. 10). Furthermore, SSA applied to that heat flux index yields a statistically significant oscillatory mode with a period of 9 years (not shown), which further supports the conjecture that air-sea coupling is important in producing the sub-decadal NAO mode.

We next examine the vertical structure of the atmospheric changes associated with the sub-decadal NAO mode. The 500 hPa geopotential height anomalies, as shown by lag-regression patterns (Fig. 11a) calculated upon the sub-decadal NAO SSA-mode reconstruction (as in Fig. 8), have a similar horizontal structure as the SLP anomalies, indicating an equivalent barotropic vertical structure and suggesting an eddy-mediated response. As in the SLP anomaly field, the changes in the centers of action of the 500 hPa height anomaly field are statistically significant. The height response goes along with statistically significant regressions in the storm track at 500 hPa (Fig. 11b), as defined by the standard deviation of the 12-hourly band-pass filtered (2.5–8 days) height anomalies. The mean storm track over the North Atlantic is centered near 45°N (Fig. 1k and contours in

Fig. 11b). During the negative NAO phase (lag −4 yr), the storm track shifts southward, during the positive NAO phase (lag 0 yr) poleward (Fig. 11b). The vertical structure of the regressions calculated from the zonally (80°W–10°E) averaged storm track reveals statistically significant changes in synoptic activity up to the 500 hPa level (Fig. 11c).

3.5 Forced atmosphere model experiments

In order to investigate the atmospheric response to the dipolar SST anomaly in more detail, we now turn to the forced integrations with the ECHAM5 atmosphere model. When the model is forced by the SST anomalies associated with the positive phase of the (observed) sub-decadal NAO mode (Fig. 7a, right panel; Fig. S4a), a statistically significant atmospheric response is simulated that is consistent with the results describe above. For example, the SLP response pattern (Fig. S4b) is rather similar to the observed pattern (Fig. 6a, right panel) and the KCM pattern (Fig. 6b, right panel) that are associated with the sub-decadal NAO variability. Furthermore, the heat flux response pattern simulated in the forced atmosphere model experiment (Fig. S4c) confirms the positive feedback postulated above on the basis of the KCM results (Fig. 8a, right panel).

Moreover, the pressure response in the forced experiment is equivalent barotropic (not shown), as it is in the KCM (Fig. 11a, right panel). Additional sensitivity experiments (not shown) reveal that it is the SST anomalies in the North Atlantic north of 25°N that are most important in driving the NAO-like atmospheric response.

It is beyond the scope of this paper to discuss the atmospheric response at great length. What is important here is that the ECHAM5 atmosphere model is sensitive to the dipolar SST anomaly associated with the sub-decadal NAO variability and reproduces the coupled model patterns. In particular, the forced atmosphere model experiment supports the existence of a positive atmosphere–ocean feedback. Atmospheric sensitivity to AMOC-related dipolar SST changes in the North Atlantic also has been recently reported from another climate model (Frankignoul et al. 2015). The limited observational data also support such an atmospheric sensitivity to mid-latitudinal SST anomalies (Bryden et al. 2014; Czaja and Frankignoul 1999; Czaja and Frankignoul 2002).

4 Summary and discussion

We have investigated the sub-decadal variability of the North Atlantic Oscillation (NAO) and of other quantities in the North Atlantic sector. Such sub-decadal variability in the North Atlantic sector is well documented from observations. The Kiel Climate Model (KCM) simulates such a North Atlantic sub-decadal variability in a millennial control run, suggesting it could be internal in nature and does not require external forcing. It is suggested on the basis of the coupled model results that the sub-decadal NAO mode is part of a coupled mode of the North Atlantic ocean–atmosphere-sea ice system. More specifically, the sub-decadal climate variability in the North Atlantic sector is the result of positive ocean–atmosphere feedback and delayed negative ocean dynamical feedback. The latter is shown by an additional coupled model integration in which the dynamical ocean model is replaced by a slab ocean model with no ocean dynamics. In that simulation, the sub-decadal NAO mode is absent. The former is supported by an uncoupled experiment with the atmospheric component (ECHAM5) of the KCM, in which the SST anomalies associated with the positive phase of the sub-decadal NAO variability drive the model.

In the KCM, a fast positive feedback on the sea surface temperature (SST) anomalies is provided by both heat flux and wind-driven ocean circulation. During a negative NAO phase, for example, the North Atlantic SST of the subpolar gyre region is anomalously warm, whereas the SST is anomalously cold southwest of the gyre. The SST anomaly pattern is reinforced by anomalous Ekman transports and the establishment of an "intergyre" gyre. The phase reversal

and (consequently) timescale of the sub-decadal mode are due to a delayed negative feedback on the SST caused by changes in the Atlantic Meridional Overturning Circulation (AMOC). In response to the changes in the overturning, a dipolar SST anomaly with opposite polarity to that prevailing during the negative phase of the sub-decadal NAO mode develops, which initiates the phase reversal of the sub-decadal NAO mode.

The coupled nature of the sub-decadal NAO mode in the model is supported by three findings. First, independent statistical analyses of SLP, SST and meridional overturning all yield a statistically significant sub-decadal mode with the same period. This unlikely is due to chance. Further, no sensitivity to the choice of the statistical parameters is found, indicating the sub-decadal mode is a robust feature of the KCM's internal variability. Second, such enhanced sub-decadal variability is not observed, neither in SLP nor in SST, in a companion coupled simulation employing a slab ocean model instead of the dynamical ocean model used in the standard KCM. Finally, third, a forced atmosphere model experiment with prescribed SST anomalies linked to the positive phase of the (observed) sub-decadal NAO variability reproduces the patterns simulated in the coupled integration of the KCM.

The observations analyzed in this study are consistent with the model results, with regard to the sub-decadal periodicity, spatial SLP and SST anomaly structure, and with respect to the relationship between the sub-decadal NAO index and dipolar SST index. For example, the KCM simulates enhanced sub-decadal variability with a period of 9 years as opposed to 8 years in the data, which is reasonably close to the observed period. Moreover, the correlation function between the sub-decadal NAO index and the sub-decadal dipolar SST index obtained from the observations is very similar to that simulated in the model, with the SST index and the NAO index exhibiting a highly significant out-of-phase correlation, indicating an enhanced meridional SST gradient goes along with a stronger NAO. This in conjunction with the uncoupled atmosphere model integration suggests an oceanic influence on the sub-decadal NAO variability such that there is a positive ocean–atmosphere feedback. We believe that this positive feedback is essential to lift the sub-decadal NAO mode to climatological importance, as previously suggested by the hybrid coupled model study of Eden and Greatbatch (2003).

The nature of air-sea interactions in the North Atlantic region is dependent on the timescale (Bjerknes 1964; Park and Latif 2005; Gulev et al. 2013; Woollings et al. 2015), and the sub-decadal timescale is an intermediate one, at which dynamical processes in both the atmosphere and the ocean may be equally important to generate SST anomalies. Here we offer a mechanism for the generation of North Atlantic sector sub-decadal climate variability that can be

tested, especially with respect to the role of the AMOC, as subsurface observations are becoming long enough to resolve the sub-decadal climate oscillation. Further, the potential role of the AMOC in providing the memory for the sub-decadal climate oscillation in the North Atlantic sector is important with regard to multiyear climate predictability. Suitably initialized climate models may exhibit skill in forecasting such sub-decadal variability months ahead. It should be kept in mind, however, that the KCM, like many other climate models, exhibits large biases in the North Atlantic region. The role of model bias in affecting sub-decadal variability in North Atlantic sector is still an open question.

Compliance with ethical standards

Conflict of interest The authors declare that they have no conflict of interest.

References

Álvarez-García F, Latif M, Biastoch A (2008) On multidecadal and quasi-decadal North Atlantic variability. J Clim 21:3433–3452. doi:10.1175/2007JCLI1800.1

Bjerknes J (1964) Atlantic air–sea interaction. Adv Geophys 10:1–82

Bryden HL, King BA, McCarthy GD, McDonagh EL (2014) Impact of a 30 % reduction in Atlantic Meridional Overturning during 2009–2010. Ocean Sci 10:683–691. doi:10.5194/os-10-683-2014

Cayan DR (1992) Latent and sensible heat flux anomalies over the northern oceans: driving the sea surface temperature. J Phys Oceanogr 22:859–881. doi:10.1175/1520-0485(1992)022<0859:LASHFA>2.0.CO;2

Cunningham SA, Roberts CD, Frajka-Williams E, Johns WE, Hobbs W, Palmer MD, Rayner D, Smeed DA, McCarthy G (2013) Atlantic Meridional Overturning circulation slowdown cooled the subtropical ocean. Geophys Res Lett 40:6202–6207. doi:10.1002/2013GL058464

Czaja A, Frankignoul C (1999) Influence of the North Atlantic SST on the atmospheric circulation. Geophys Res Lett 26:2969–2972. doi:10.1029/1999GL900613

Czaja A, Frankignoul C (2002) Observed impact of Atlantic SST anomalies on the North Atlantic Oscillation. J Clim 15:606–623. doi:10.1175/1520-0442(2002)015<0606:OIOASA>2.0.CO;2

Czaja A, Marshall J (2001) Observations of atmosphere-ocean coupling in the North Atlantic. Q J R Meteorol Soc 127:1893–1916. doi:10.1256/smsqj.57602

Deser C, Blackmon ML (1993) Surface climate variations over the North Atlantic ocean during winter: 1900–1989. J Clim 6:1743–1753. doi:10.1175/1520-0442(1993)006<1743:SCVOTN>2.0.CO;2

Drews A, Greatbatch RJ, Ding H, Latif M, Park W (2015) The use of a flow field correction technique for alleviating the North Atlantic cold bias with application to the Kiel Climate Model. Ocean Dyn 65:1079–1093. doi:10.1007/s10236-015-0853-7

Eden C, Greatbatch RJ (2003) A damped decadal oscillation in the North Atlantic Climate System. J Clim 16:4043–4060. doi:10.1175/1520-0442(2003)016<4043:ADDOIT>2.0.CO;2

Frankignoul C, Gastineau G, Kwon Y (2015) Wintertime atmospheric response to North Atlantic ocean circulation variability in a climate model. J Clim. doi:10.1175/JCLI-D-15-0007.1

Fye FK, Stahle DW, Cook ER, Cleaveland MK (2006) NAO influence on sub-decadal moisture variability over central North America. Geophys Res Lett 33:L15707. doi:10.1029/2006GL026656

Gulev SK, Latif M, Keenlyside N, Park W, Koltermann KP (2013) North Atlantic ocean control on surface heat flux on multidecadal timescales. Nature 499:464–467. doi:10.1038/nature12268

Hurrell JW (1995) Decadal trends in the North Atlantic Oscillation: regional temperatures and precipitation. Science 269:676–679. doi:10.1126/science.269.5224.676

Hurrell JW, Kushnir Y, Ottersen G, Visbeck M (2003) An overview of the North Atlantic Oscillation. In: Hurrell JW, Kushnir Y, Ottersen G, Visbeck M (eds) The North Atlantic Oscillation: climate significance and environmental impact. American Geophysical Union, Washington. doi:10.1029/134GM01

Knight JR, Allan RJ, Folland CK, Vellinga M, Mann ME (2005) A signature of persistent natural thermohaline circulation cycles in observed climate. Geophys Res Lett 32:L20708. doi:10.1029/2005GL024233

Leith CE (1973) The standard error of time-average estimates of climatic means. J Appl Meteorol 12(6):1066–1068. doi:10.1175/1520-0450(1973)012<1066:TSEOTA>2.0.CO;2

Marshall J, Johnson H, Goodman J (2001) Study of the interaction of the North Atlantic Oscillation with ocean circulation. J Clim 14:1399–1421. doi:10.1175/1520-0442(2001)014<1399:ASOTIO>2.0.CO;2

Park W, Latif M (2005) Ocean Dynamics and the Nature of Air-Sea Interactions over the North Atlantic at Decadal Time Scales. J Clim 18:982–995. doi:10.1175/JCLI-3307.1

Park W, Latif M (2008) Multidecadal and multicentennial variability of the meridional overturning circulation. Geophys Res Lett 35:L22703. doi:10.1029/2008GL035779

Park W, Keenlyside N, Latif M, Ströh A, Redler R, Roeckner E, Madec G (2009) Tropical Pacific climate and its response to global warming in the Kiel Climate Model. J Clim 22:71–92. doi:10.1175/2008JCLI2261.1

Saravanan R, McWilliams JC (1997) Stochasticity and spatial resonance in interdecadal climate fluctuations. J Clim 10:2299–2320. doi:10.1175/1520-0442(1997)010<2299:SASRII>2.0.CO;2

Saravanan R, McWilliams JC (1998) Advective ocean–atmosphere interaction: an analytical stochastic model with implications for decadal variability. J Clim 11:165–188. doi:10.1175/1520-0442(1998)011<0165:AOAIAA>2.0.CO;2

Smeed D, McCarthy G., Rayner D., Moat BI, Johns WE, Baringer MO, Meinen CS (2015) Atlantic meridional overturning circulation observed by the RAPID-MOCHA-WBTS (RAPID-Meridional Overturning Circulation and Heatflux Array-Western Boundary Time Series) array at 26 N from 2004 to 2014. British Oceanographic Data Centre—Natural Environment Research Council, UK

Sutton RT, Allen MR (1997) Decadal predictability of North Atlantic sea surface temperature and climate. Nature 388:563–567. doi:10.1038/41523

Vautard R, Ghil M (1989) Singular spectrum analysis in nonlinear dynamics, with applications to paleoclimatic time series. Phys D 35:395–424. doi:10.1016/0167-2789(89)90077-8

Visbeck M, Hurrel JW, Polvani L, Cullen HM (2001) The North Atlantic Oscillation: past, present, and future. Proc Natl Acad Sci USA 98:12876–12877. doi:10.1073/pnas.231391598

Woollings T, Gregory JM, Pinto JG, Reyers M, Brayshaw DJ (2015) Contrasting interannual and multidecadal NAO variability. Clim Dyn 45:539–556. doi:10.1007/s00382-014-2237-y